

Cold atmospheric plasma for preventing infection of viruses that use ACE2 for entry

Peiyu Wang^{a,b,c,d,1}, Renwu Zhou^{e,f,1}, Rusen Zhou^{e,f,1}, Wenshao Li^g, Janith Weerasinghe^e, Shuxiong Chen^h, Bernd H. A. Rehm^h, Liqian Zhaoⁱ, Francesca D. Frentiu^{c,j}, Zhifa Zhang^a, Kexin Yan^k, Mary Lor^k, Andreas Suhrbier^{k,l}, Derek Richard^{c,d}, Erik W. Thompson^{c,d}, Kostya (Ken) Ostrikov^e, and Xiaofeng Dai^{a,1,2}

^aWuxi School of Medicine, Jiangnan University, Wuxi 214122, China

^bState Key Laboratory of Molecular Vaccinology and Molecular Diagnostics & Center for Molecular Imaging and Translational Medicine, School of Public Health, Xiamen University, Xiamen 361102, China.

^cSchool of Biomedical Sciences, Queensland University of Technology, Brisbane 4059, Australia

^dTranslational Research Institute, Woolloongabba, Queensland 4102, Australia

^eSchool of Chemistry and Physics, Queensland University of Technology, Brisbane 4000, Australia

^fSchool of Chemical and Biomolecular Engineering, University of Sydney, Sydney, Australia

^gSchool of Biology and Environmental Science, Queensland University of Technology, Brisbane 4000, Queensland, Australia

^hCentre for Cell Factories and Biopolymers, Griffith Institute for Drug Discovery, Griffith University, Nathan, QLD 4111, Australia

ⁱThe First School of Clinical Medicine, Southern Medical University, Guangzhou 510515, China

^jCentre for Immunology and Infection Control, Queensland University of Technology, Brisbane 4059, Australia

^kQIMR Berghofer Medical Research Institute, Herston QLD 4006, Australia

^lAustralian Infectious Disease Research Centre, GVN Center of Excellence, Brisbane, Queensland, Australia.

¹These authors contributed equally to this work.

²To whom correspondence may be addressed. Email: xiaofeng.dai@jiangnan.edu.cn

Table S1. Q-TOF/MS analysis of PhaC-SARS-CoV-2 antigen fusion proteins.

Protein/Protein sequence*	Peptide fragments assigned to the various protein regions
PhaC-RBD (89.9 kDa)	
MATGK GAAASTQEGKSQPFKVT PGPFDPATWLEWSRQWOGTEGNGHAA AASGIPGLDALAGVKIAPAQLGDIQQRVMKDFSAWQAMAEGKAEATG PLHRRFAGDAWRNLPYRFAAAFYLLNARALTELADAVEADAKTR QR IRFAISQWVDAMSPANFLATNPEAQRLLIESGGESLRAGVRNMMEDLTR GKISQTDSEAFEVGRNVAVTEGAVVFENEYFQLQYKPLTDKVHARPLL MVPPCINKYYILDLOPESSLVRHVVEQGHTVFLVSWRNPDASMAGSTWD DYIEHAAIR AIEVAR DISGQDKINVLGFCVGGTIVSTALAVLAARGEHPAA SVTLLTLLDFADTGILDFVDEGHVQLREATLGGGAGAPCALLRGLLEL ANTFSFLRPNDLVWNYVVDNYLK GNT TPVFDLLFWNGDATNLPGPWYC WYLRHTYLQNELKVPVKLTVCVGPVVDLASIDVPTYIYGSREDHIVPWA AYASTALLANKLR FVLGASGHIAGVINPPAK NKRSHWTNDALPESPOQW LAGAIEHHGSWW PDWTAWLAGQAGAKRAAPANYGNARYR AIEPAPGR YVKAKA-Linker- RVQPTESIVR FPNITNLC PFGEVENATRFASVYAWNRKRISNCVADYSVL LYNSASFSTFKCYGV SPTKLNDLC FTNVYADSFVIRGDEVRQIAPGQTGKI ADYNYKLPDDFTGC VIAWNSNNLDSK VGGNYNYLYRFRKSNLKPFFER DISTEIQAGST PCNG VEGFNCYFPLQSY GFQPTNGVGYQPYR VVLSFE LLHAPATVCGPKK	PhaC: G6-R141, F146-R299, D306-F318, L329-K413, G434-W536, P549-R573, A576-R583 RBD: I624-T677, F684-R746, K750-C772, G788-K821
RBD-PhaC-N protein (135.4 kDa)	
MRVQPTESIVR FPNITNLC PFGEVENATRFASVYAWNRKRISNCVADYSVL LYNSASFSTFKCYGV SPTKLNDLC FTNVYADSFVIRGDEVRQIAPGQTGKI ADYNYKLPDDFTGC VIAWNSNNLDSK VGGNYNYLYRFRKSNLKPFFER DISTEIQAGST PCNG VEGFNCYFPLQSY GFQPTNGVGYQPYR VVLSFE LLHAPATVCGPKK-Linker- ATGKGAAASTQEGKSQPFKVT PGPFDPATWLEWSRQWOGTEGNGHAA ASGIPGLDALAGVKIAPAQLGDIQQRVMKDFSAWQAMAEGKAEATG F LHRRFAGDAWRNLPYRFAAAFYLLNARALTELADAVEADAK TRQRI RFAISQWVDAMSPANFLATNPEAQRLLIESGGESLRAGVRNMMEDLTRG KISQTDSEAFEVGR NVAVTEGAVVFENEYFQLQYKPLTDKVHARPLL VPPCINKYYILDLOPESSLVRHVVEQGHTV FLVSWRNPDASMAGSTWDD YIEHAAIR AIEVAR DISGQDKINVLGFCVGGTIVSTALAVLAARGEHPAA S VTLLTLLDFADTGILDFVDEGHVQLREATLGGGAGAPCALLRGLLEL A NTFSFLRPNDLVWNYVVDNYLK GNT TPVFDLLFWNGDATNLPGPWYC WYLRHTYLQNELKVPVKLTVCVGPVVDLASIDVPTYIYGSREDHIVPWA AYASTALLANKLR FVLGASGHIAGVINPPAK NKRSHWTNDALPESPOQW LAGAIEHHGSWW PDWTAWLAGQAGAKRAAPANYGNARYR AIEPAPGR YVKAKA-Linker- SDNGPQNQRNAPR TFGGPSDSTGSNQNGERSGARSKORRPOGLPNNTAS WFTALTQHGKEDLK FPRGQGV PINTNSSPDDQIGY YR ATTRIRGGDGK MKDLS PRWYFY YLTGTGPEAGL PYGANKDGIIWVATEGALNTPK DHIGTR NPANNA AI VLQ LQ PGTTL PKGFY AE GS RGG SQASSRSSRSRNSRN STPG SSRGT SPARMAG NGGDAALALLLLDRL NQLESKMSGK GQQQ QGTIVTK K SAEA E SKKPRQ KRTAT KAYNY TQAF GRRGPEQTQGNF GDQELIR Q GTD YKHWPQ IAQFAPSASAFFGMSRIGMEVTPSGTWLTYTGAIKLDDKDPNT K DQVILLNKHIDAYKTFPPTEPKDKK KADE TQALPORQK QQ VTLL PAADLDDFSK LQOQSMSSADSTQA	RBD: M1-R11, I15-K39, I41-K69, A81-R137, K141-P162, G179-R192 PhaC: A218-K355, F362-R423, V451-V488, N495-R515, G552-F610, Y653-K671, L681-K714, F717-K734, R778-R788, A791-R800 N protein: I839-R913, M925-R931, Y936-K967, N974-R1001, M1034-R1117, I1144-K1194, K1198-R1209, K1212-A1243

Table S2. Genes differentially expressed on SARS-CoV-2 infection in human bronchial epithelial (NHBE) cells using GSE147507.

Gene name	log2FoldChange	p value	p_adjust	Direction
CCL20	3.14396175	3.26E-80	3.91E-76	up
SAA2	2.42248925	3.4E-79	2.04E-75	up
SAA1	2.22177266	8.61E-58	3.44E-54	up
S100A8	1.86933142	2.92E-53	6.99E-50	up
IL36G	2.73218605	2.37E-53	6.99E-50	up
TNFAIP3	1.61148647	2.41E-52	4.82E-49	up
SPRR2D	2.97919497	1.76E-51	3.01E-48	up
INHBA	1.81922735	5.18E-51	7.76E-48	up
C3	1.50866591	4.32E-46	5.76E-43	up
KRT6B	1.54827214	9.85E-46	1.18E-42	up
ICAM1	1.86166523	1.76E-45	1.76E-42	up
TNIP1	1.26402353	1.71E-45	1.76E-42	up
CFB	1.8548093	2.18E-44	2.01E-41	up
CXCL1	1.4172731	2.58E-42	2.21E-39	up
SOD2	1.51945874	3.03E-38	2.42E-35	up
MX1	2.50985094	1.38E-36	1.04E-33	up
S100A9	1.10738825	5.9E-36	4.16E-33	up

ZC3H12A	1.67390106	1.13E-34	7.51E-32	up
C15orf48	1.23597139	2.1E-31	1.32E-28	up
LIF	1.30739366	4.38E-31	2.63E-28	up
CXCL5	3.48535834	7.82E-31	4.47E-28	up
RHCG	1.34872189	8.28E-31	4.52E-28	up
HBEGF	1.29188055	1.31E-30	6.84E-28	up
SLC6A14	1.21811219	2.83E-29	1.42E-26	up
IRF9	1.25047085	9.16E-29	4.39E-26	up
IL1B	1.06251861	4.02E-28	1.85E-25	up
SPRR2A	1.68768801	3.1E-27	1.38E-24	up
TNFAIP2	1.54932822	1.73E-26	7.39E-24	up
IL6	2.92646346	2.12E-26	8.77E-24	up
MMP9	2.28503359	1.42E-25	5.66E-23	up
IL32	1.22070157	1.7E-24	6.6E-22	up
SERPINA3	1.46770413	9.92E-24	3.72E-21	up
PDZK1IP1	2.4278506	2.79E-23	1.02E-20	up
OAS3	1.31779675	2.92E-23	1.03E-20	up
PLAT	1.39509077	1.09E-22	3.75E-20	up
CSF3	4.85032851	1.15E-22	3.82E-20	up
BIRC3	1.66152604	1.74E-22	5.64E-20	up
OAS2	1.2662775	2.84E-22	8.98E-20	up
OAS1	1.6954135	2.56E-19	7.68E-17	up
CXCL2	1.39127199	5.35E-19	1.57E-16	up
IRAK2	1.59984891	1.5E-18	4.19E-16	up
PGLYRP4	2.03747854	6.51E-18	1.74E-15	up
CXCL3	2.23021571	2.93E-17	7.64E-15	up
MAFF	1.13326426	6.1E-17	1.56E-14	up
SPRR2E	3.59793307	1.92E-16	4.8E-14	up
IL1A	1.07203604	7.41E-16	1.74E-13	up
HEPHL1	1.30788314	1.43E-15	3.29E-13	up
XAF1	2.53063831	1.98E-15	4.48E-13	up
IVL	1.03806572	5.92E-15	1.29E-12	up
IFI27	2.89474326	1.2E-14	2.58E-12	up
CIQTNF1	1.87212235	1.52E-14	3.19E-12	up
CSF2	2.97894511	5.15E-13	1.05E-10	up
IFITM10	-1.5710814	1.63E-12	3.27E-10	down
BCL2A1	2.28834639	2.52E-12	4.95E-10	up
IFITM1	1.6147879	1.18E-11	2.14E-09	up
EDN1	1.0605424	3.5E-10	5.83E-08	up
PI3	1.80075642	1.75E-09	2.56E-07	up
PDGFB	1.01434311	1.8E-09	2.61E-07	up
MX2	2.21993955	2.83E-09	3.99E-07	up
SOCS3	1.0373848	2.35E-08	0.00000285	up
VNN1	1.883174	3.53E-08	0.00000412	up
KRT4	1.01298875	4.22E-08	0.00000482	up
TYMP	1.04040175	4.89E-08	0.00000553	up
VTCN1	-1.0742581	6.03E-08	0.00000676	down
MYLK	-1.4288626	6.57E-08	0.00000714	down
CXCL14	-1.4485315	6.6E-08	0.00000714	down
METTL7A	-1.0357868	1.44E-07	0.0000149	down
ADAM8	1.01426869	1.94E-07	0.0000192	up
ITGB3	1.19799377	9.47E-07	0.0000836	up
CYP27B1	1.20606261	0.00000133	0.000113	up
TNFSF14	1.99248464	0.0000014	0.00011664	up
RND1	1.51644941	0.00000195	0.00015935	up
IRF7	1.57303744	0.00000278	0.00021648	up
TNF	1.80716236	0.00000394	0.00029508	up

MYEOV	1.28223564	0.00000483	0.0003513	up
KRT24	1.79683578	0.00000869	0.00059256	up
MAP7D2	-1.3954685	0.00000867	0.00059256	down
NID1	-1.2290109	0.00000976	0.00065773	down
HELZ2	1.01051942	0.0000232	0.00142745	up
VNN3	2.74162665	0.000026	0.00157425	up
MRGPRX3	1.95888146	0.000027	0.00162927	up
IFI6	2.34449344	0.0000344	0.00202474	up
PPARGC1A	-1.0471203	0.0000363	0.00210458	down
TRIML2	1.39749281	0.0000463	0.00257094	up
TLR2	1.05056807	0.0000486	0.00268432	up
BST2	1.29187352	0.0000521	0.0028396	up
MAP3K8	1.06163063	0.0000574	0.00308576	up
EPSTI1	1.04447947	0.0000608	0.00324312	up
ATG9B	-1.1310397	0.0000614	0.0032589	down
GBP5	1.83077415	0.00012273	0.00603509	up
CXCL6	1.73041085	0.00012274	0.00603509	up
NANOS1	-1.5176398	0.00012404	0.00607391	down
S100A12	1.2238146	0.00017339	0.00809391	up
LTB	1.6385608	0.00018339	0.00849455	up
STAT5A	1.11992847	0.00018495	0.00853402	up
STON1	-1.5080852	0.00019045	0.00872086	down
IFI44L	2.27820079	0.00028877	0.01246185	up
MMP13	1.09446902	0.00030101	0.01285144	up
ZNF488	-1.1399958	0.00037534	0.01516131	down
CYP4F3	-1.0730949	0.00041372	0.01632709	down
FAM167A	1.09674174	0.00082419	0.02843076	up
P2RY6	1.13520504	0.00100864	0.03279294	up
RBM20	-1.5835055	0.00127333	0.03967835	down
PSMB9	1.01490868	0.00151653	0.04497961	up
C6orf223	1.15507754	0.00156657	0.04601422	up

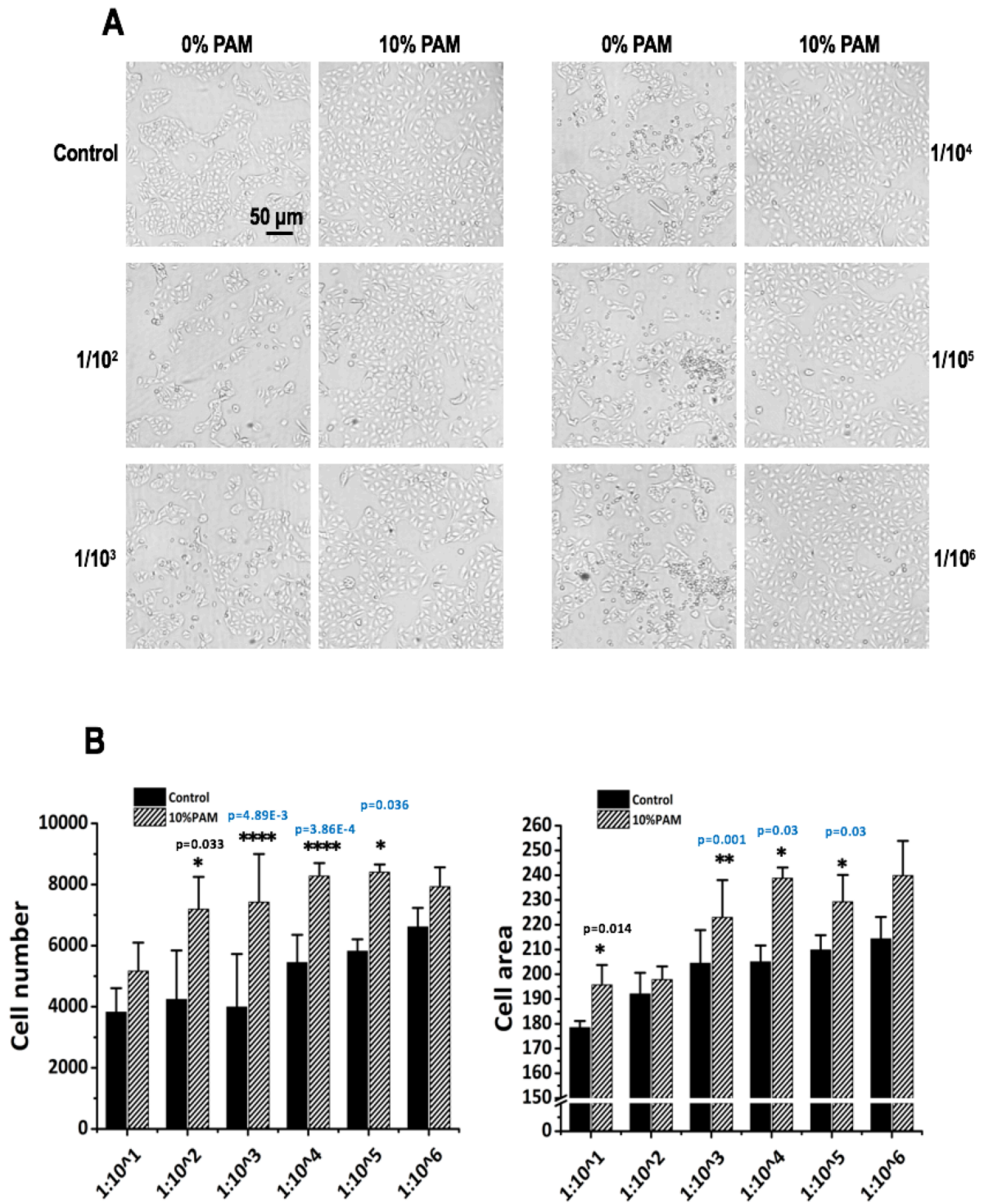
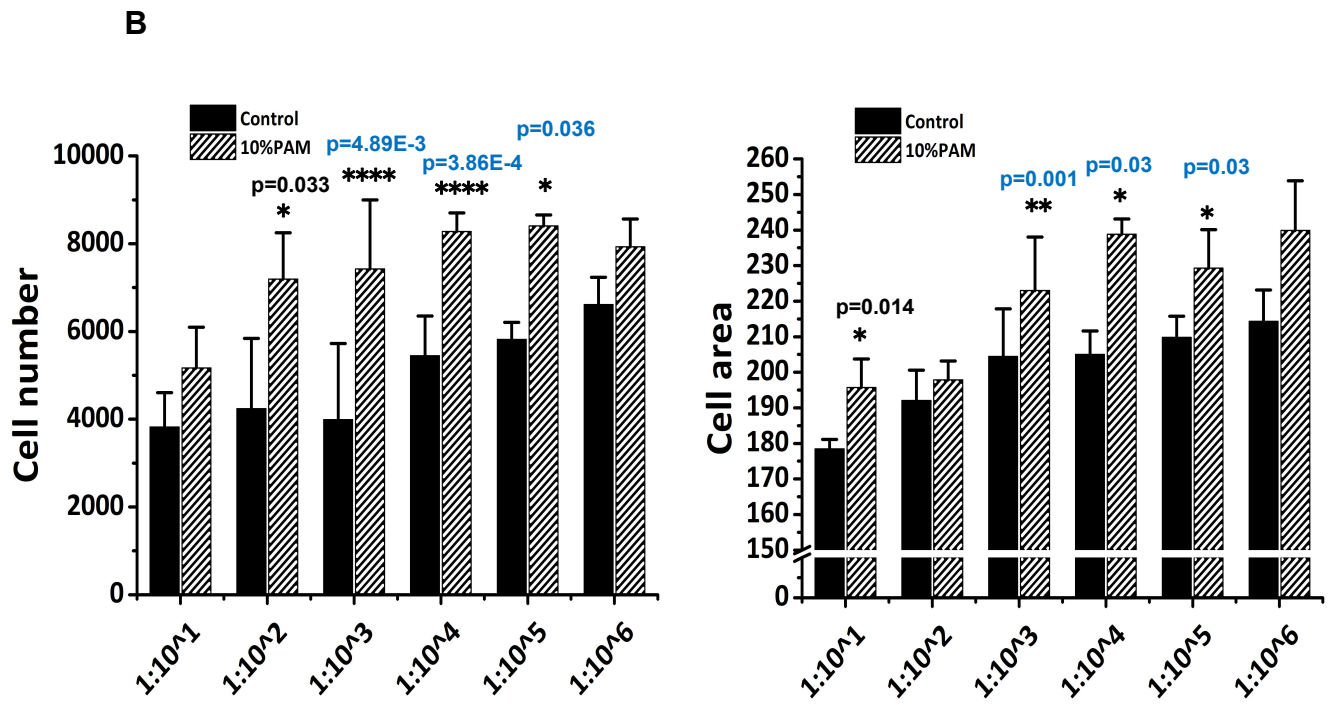
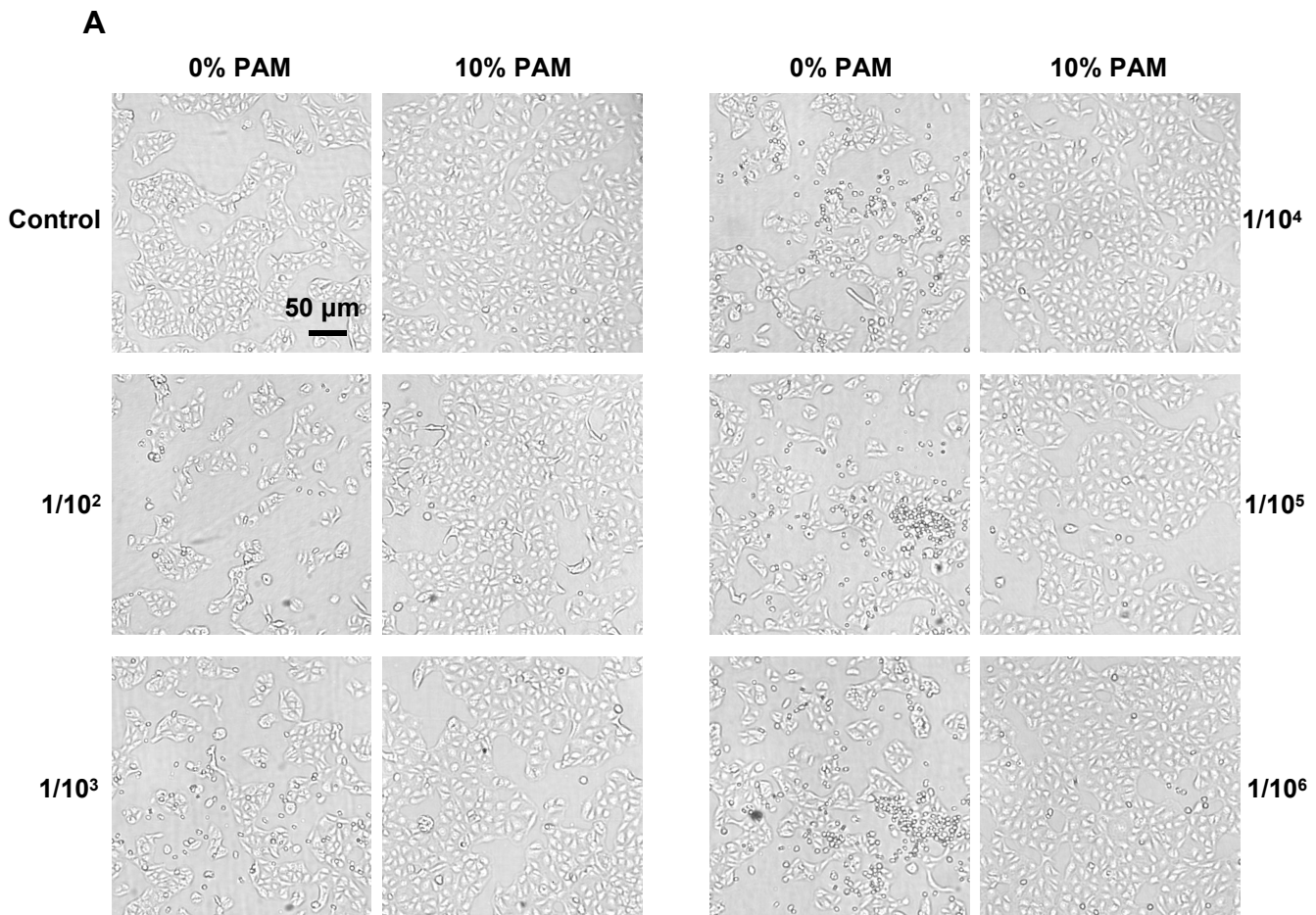


Figure S1. Images showing the preventive role of CAP on Vero E6 cells against SARS-CoV-2 infection. (A) Phase contrast images of cells infected with different dilution of 10E6.79 TCID₅₀/mL virus, without (0% PAM) or with (10% PAM) pre-treatment, prior to virus addition. Cell morphology alterations were observed 1 day after exposing cells to 10 min 10% PAM treatment. (B) Graphs show quantification of cell number and cell area, conducted using IN Carta Analysis, with statistical analysis (n=4) using t-test assuming unequal variance or non-parametric tests, as appropriate. P values are shown above the bars in red if significant. Images of cells infected with SARS-CoV-2 at different dilution folds, without (Control) and with 10% PAM treatment prior to virus addition (10% PAM). Cell morphology alterations were observed 1 day after exposing cells to 10 min 10% PAM treatment. Quantification of cell number and cell area were conducted using IN Carta Analysis.



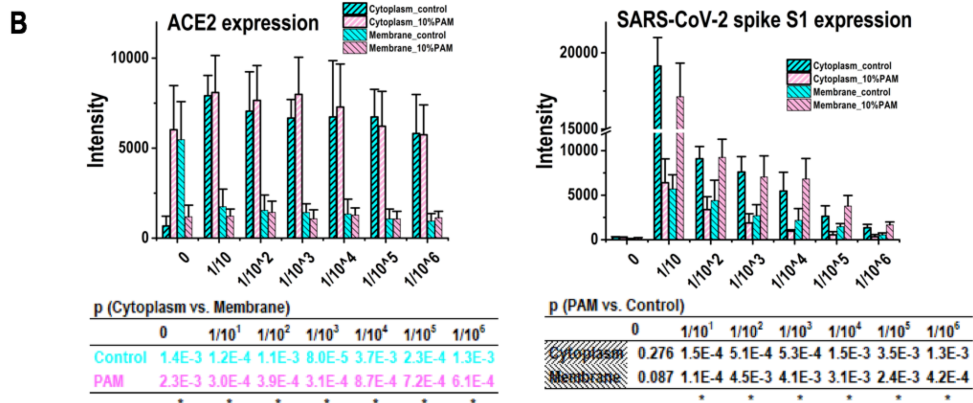
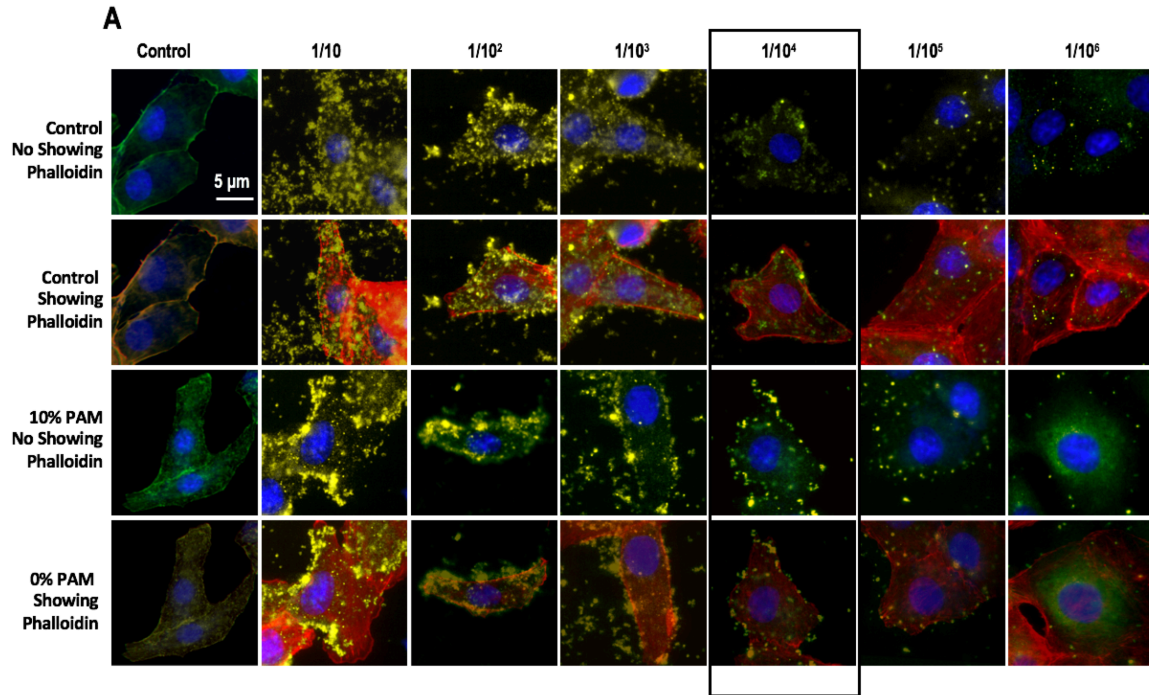
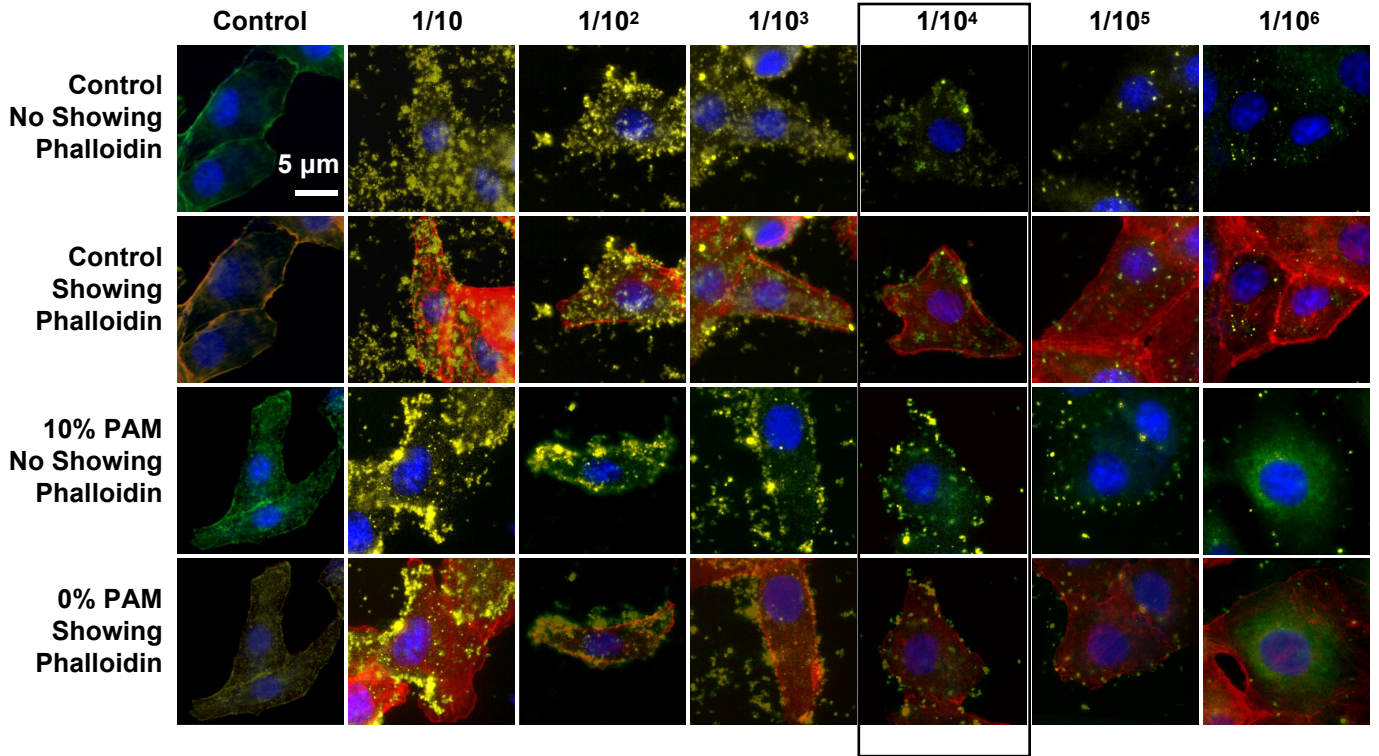
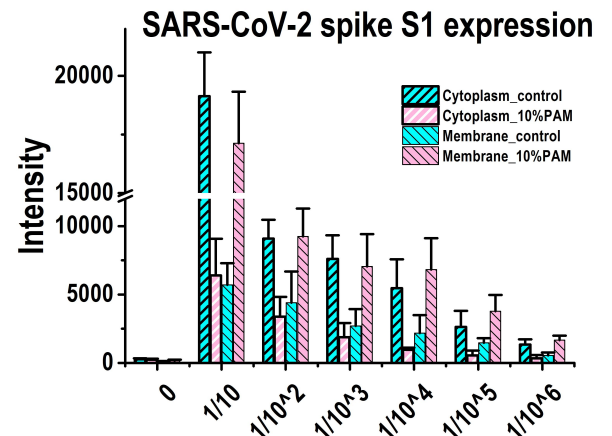
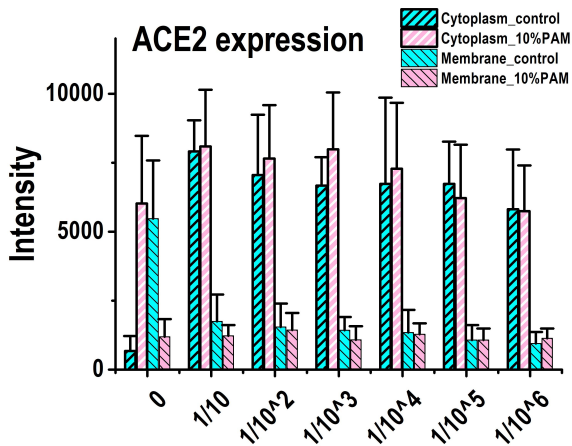


Figure S2. Additional images showing the preventive role of CAP on Vero E6 cells against SARS-CoV-2 infection. (A) Immunofluorescence for ACE2 (green) or SARS-CoV-2 viral particles (yellow) and staining for actin filaments (phalloidin; red) or DNA (Hoechst 33342; blue), showing extracellular virus on Vero E6 cells that underwent 0% PAM or 10% PAM pre-treatment prior to the infection with different dilution of 10E6.79 TCID50/mL SARS-CoV-2 virus. (B) Phalloidin staining of actin was used as a reference against which the number and intensity of stained particles were counted. Graphs show quantification of ACE2 staining or SARS-CoV-2 virus particles, conducted using IN Carta Analysis, and represent mean \pm SD of the data. Significance was assessed using Student's T-test and p-values for each comparison (0% vs 10% PAM) are shown in the Tables below each graph. n=4.

A



B



p (Cytoplasm vs. Membrane)

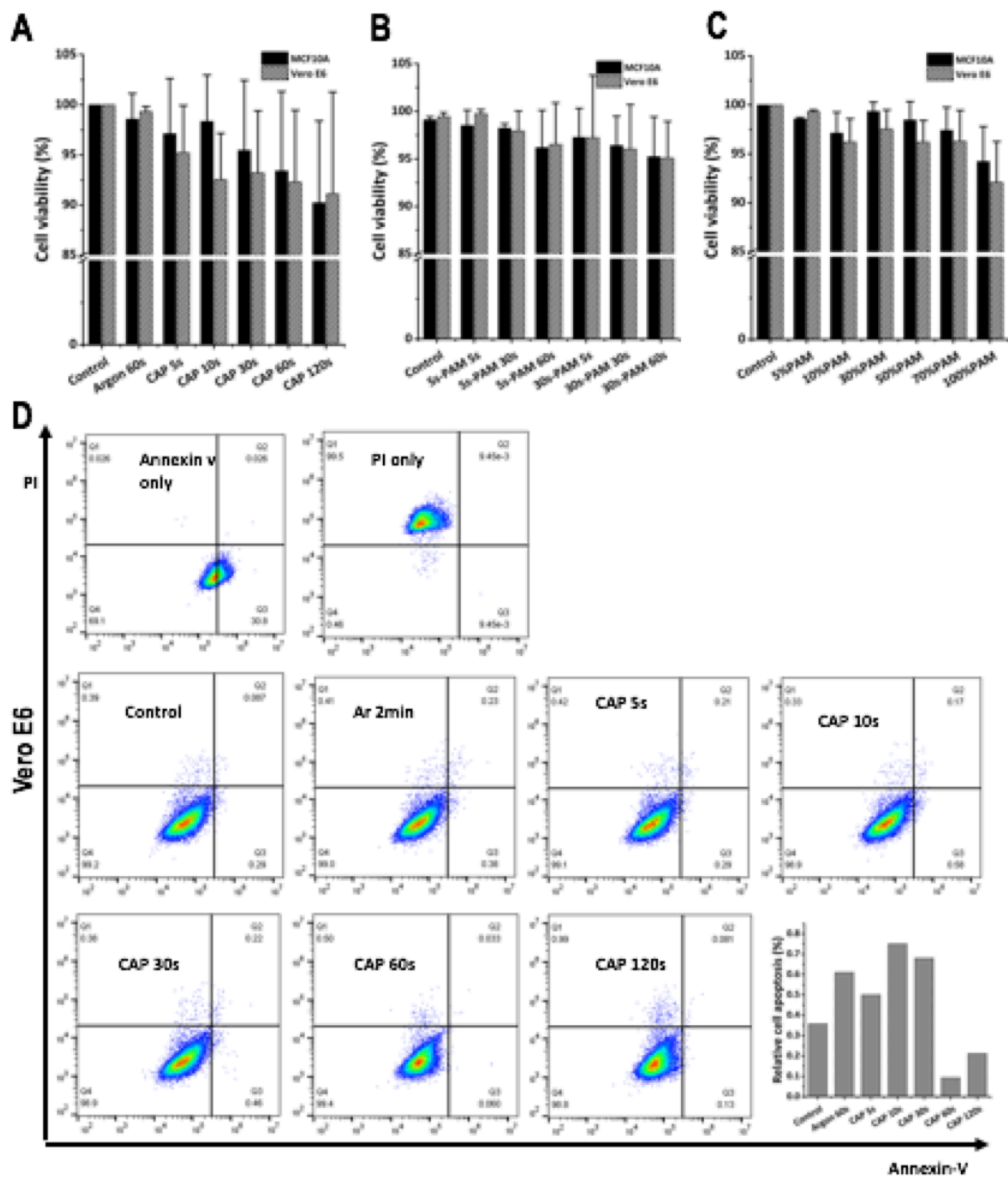
	0	1/10 ¹	1/10 ²	1/10 ³	1/10 ⁴	1/10 ⁵	1/10 ⁶
Control	1.4E-3	1.2E-4	1.1E-3	8.0E-5	3.7E-3	2.3E-4	1.3E-3
PAM	2.3E-3	3.0E-4	3.9E-4	3.1E-4	8.7E-4	7.2E-4	6.1E-4

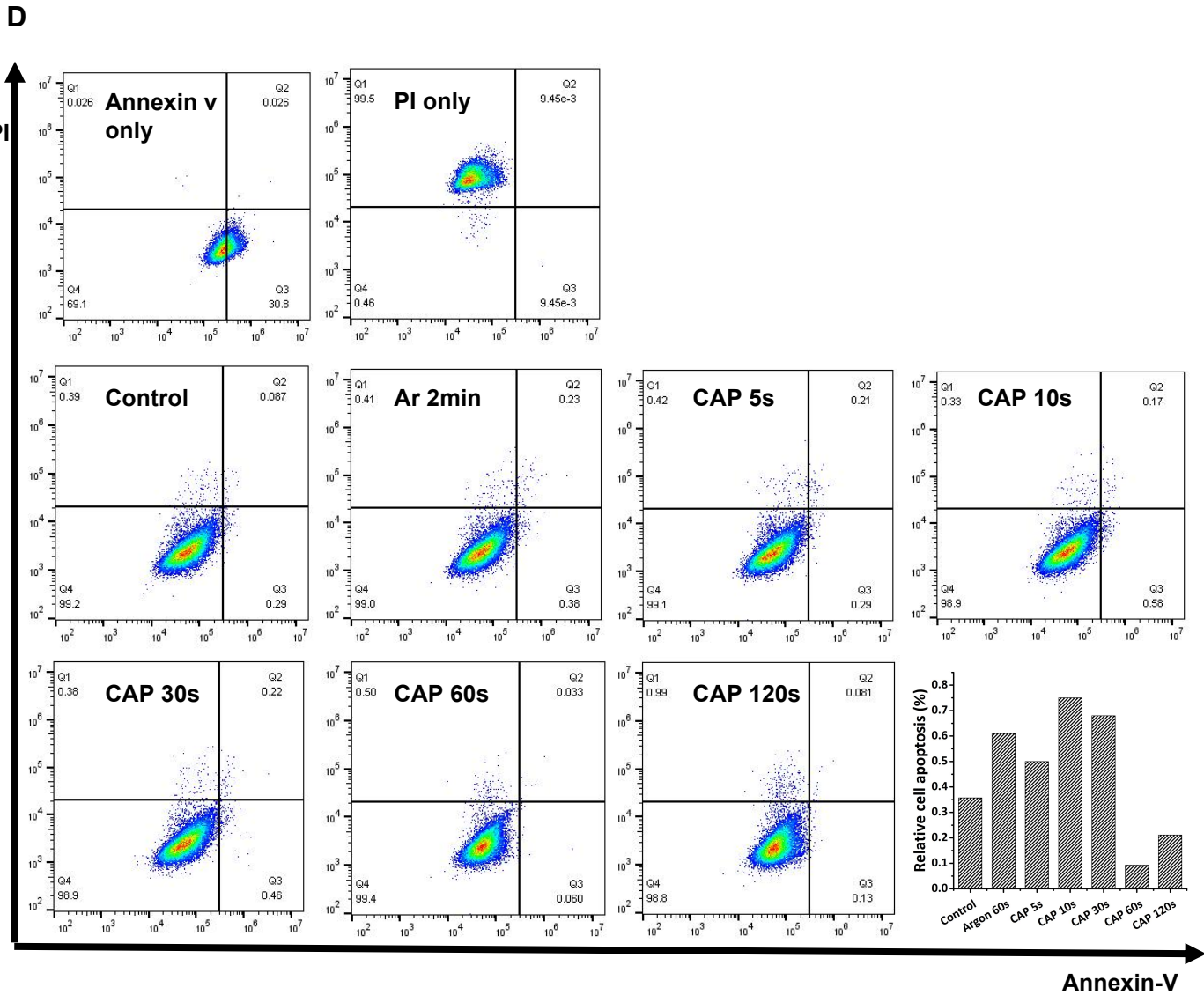
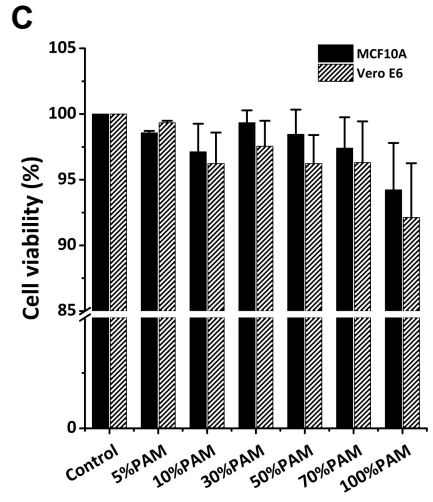
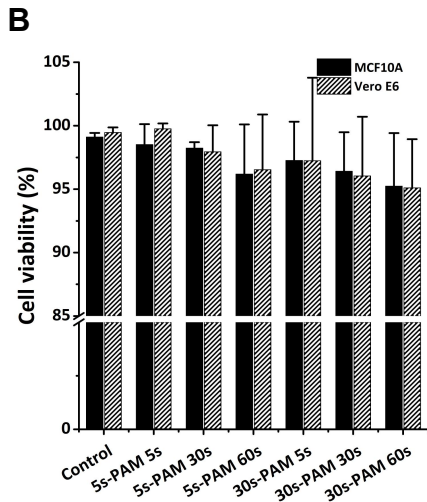
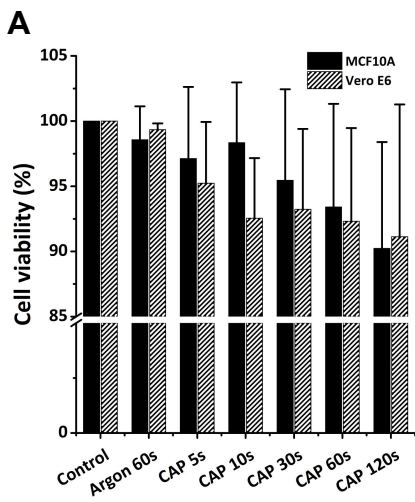
* * * * * * *

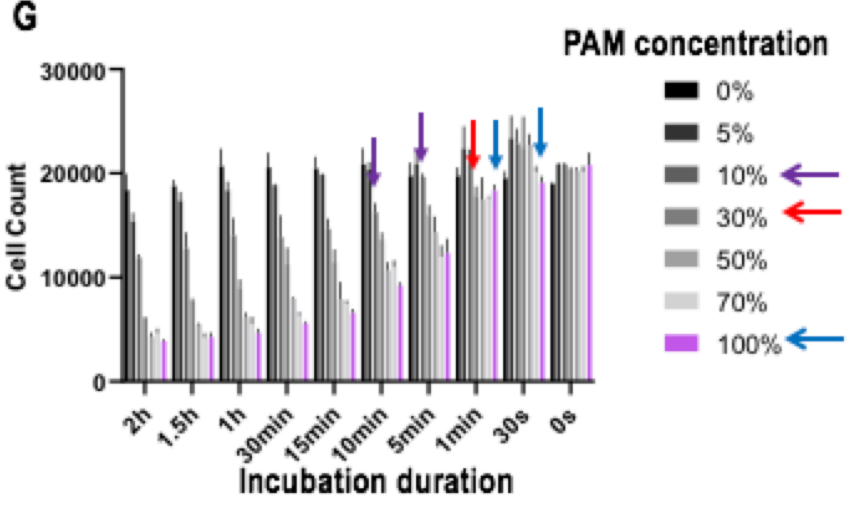
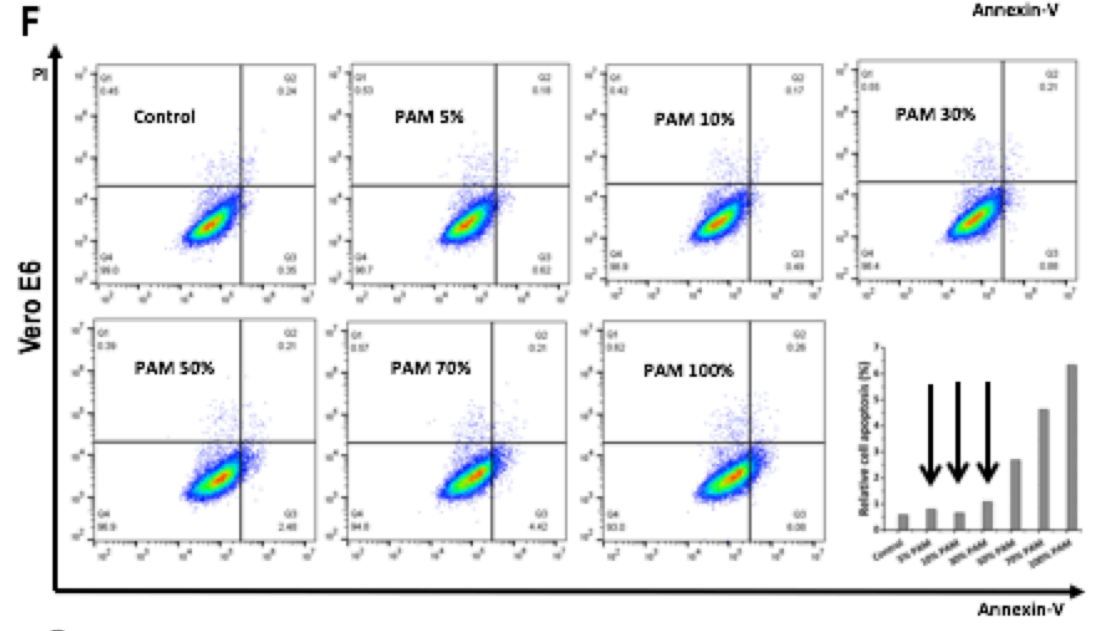
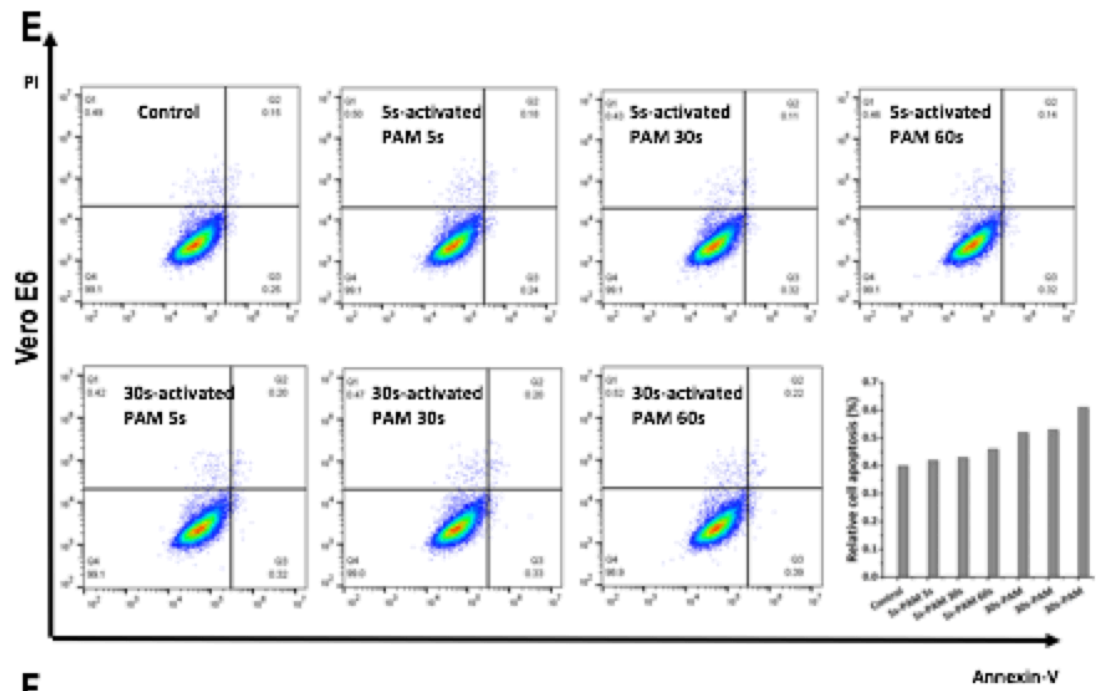
p (PAM vs. Control)

	0	1/10 ¹	1/10 ²	1/10 ³	1/10 ⁴	1/10 ⁵	1/10 ⁶
Cytoplasm	0.276	1.5E-4	5.1E-4	5.3E-4	1.5E-3	3.5E-3	1.3E-3
Membrane	0.087	1.1E-4	4.5E-3	4.1E-3	3.1E-3	2.4E-3	4.2E-4

* * * * * *







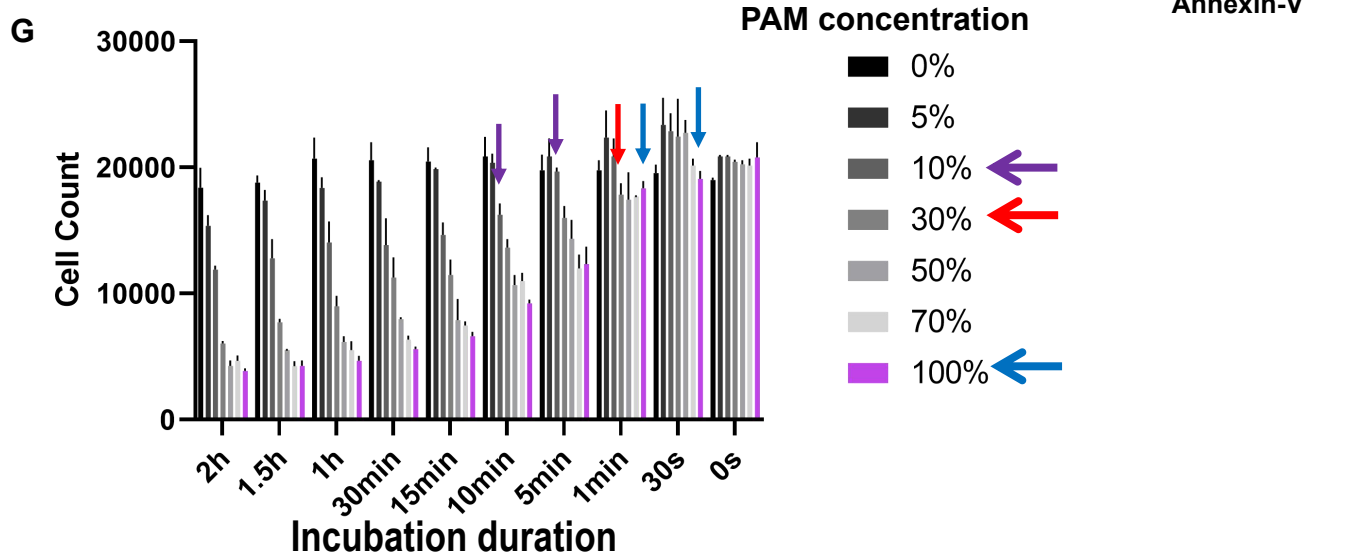
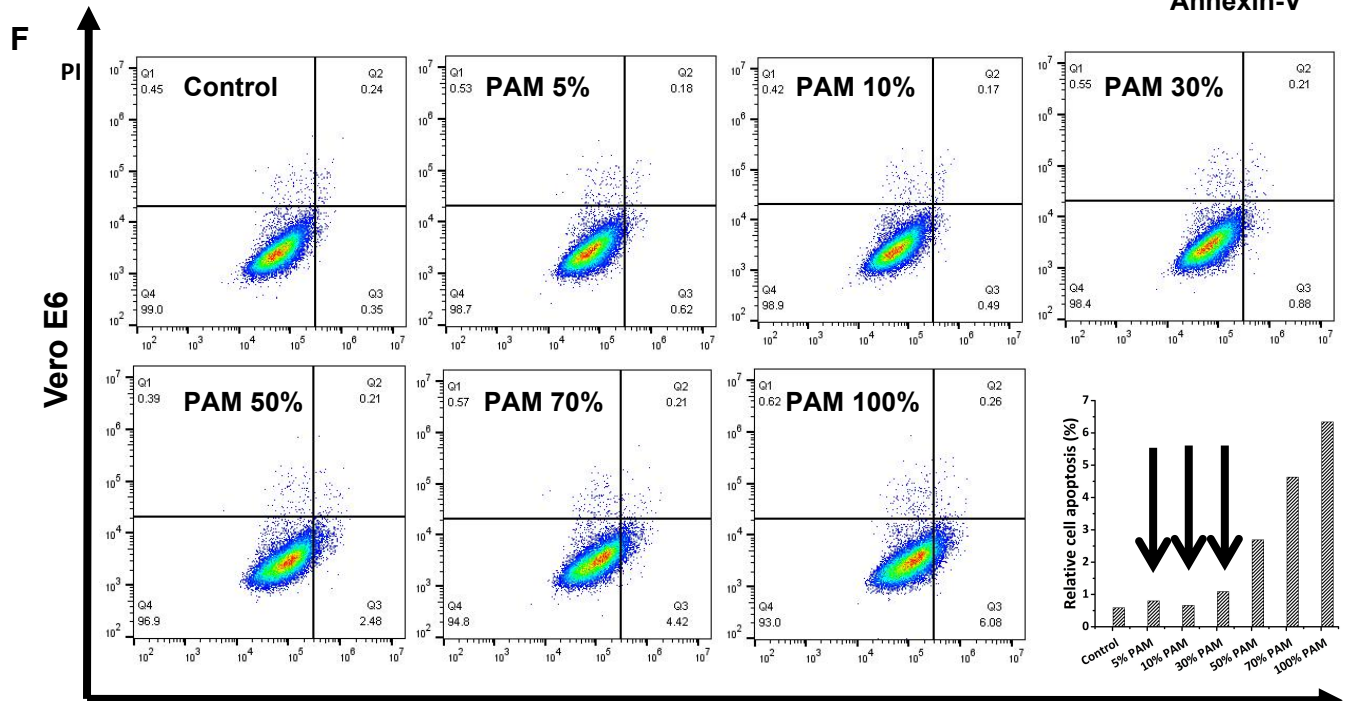
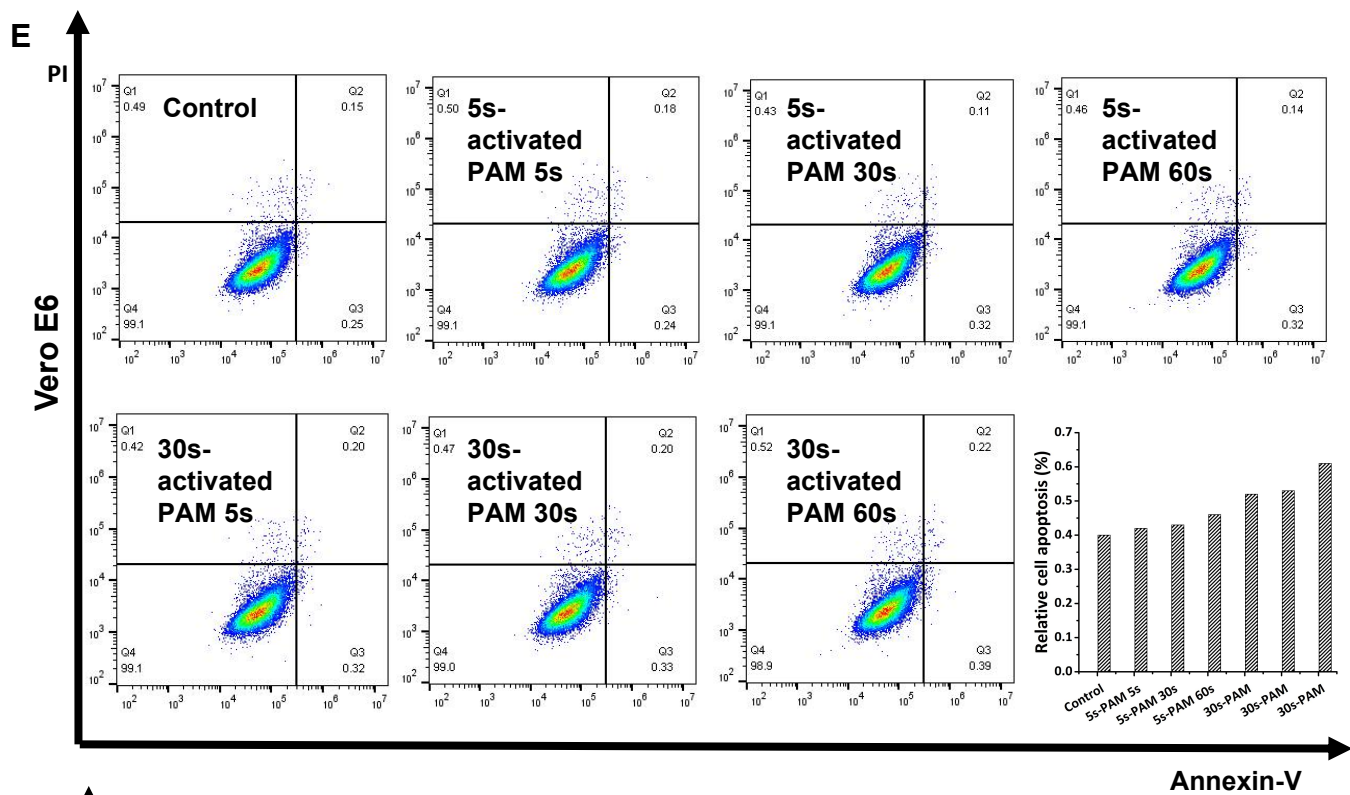


Figure S3. Additional images showing the effects of different CAP and PAM concentrations on cell viability and apoptosis. Viability of MCF10A and Vero E6 cells in response to (A) direct CAP treatment at different treatment durations, (B) indirect PAM treatment activated by CAP for different treatment durations, and (C) indirect 10-min activated PAM treatment diluted into different concentrations. Apoptosis of Vero E6 cells in response to (D) different CAP treatment durations, (E) different CAP exposure time activated PAM for different treatment durations, and (F) 1 min CAP exposure activated PAM diluted into different concentrations. (G) Vero E6 cell counts under PAM indirect treatment at different diluted concentrations and for different treatment durations.

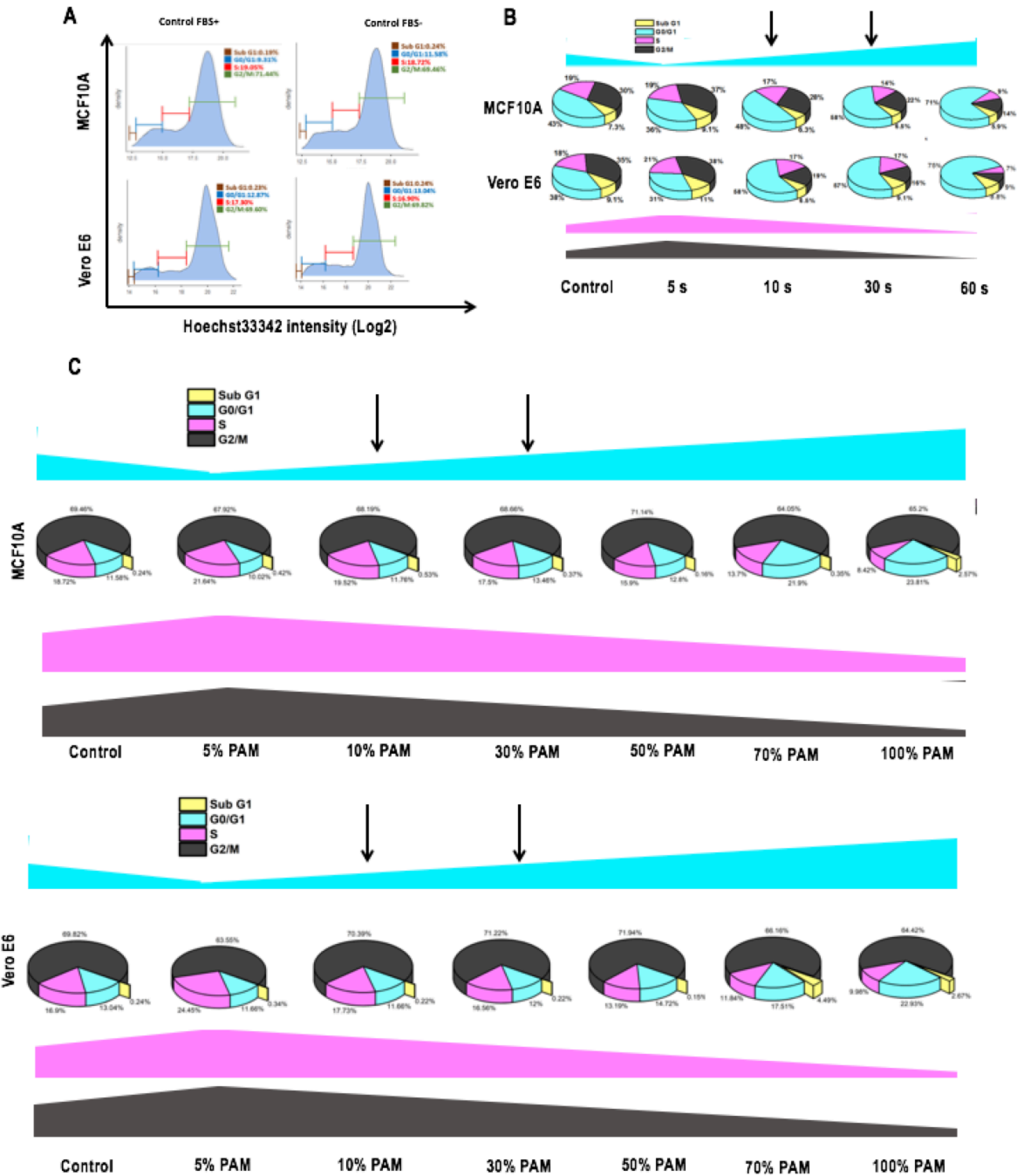
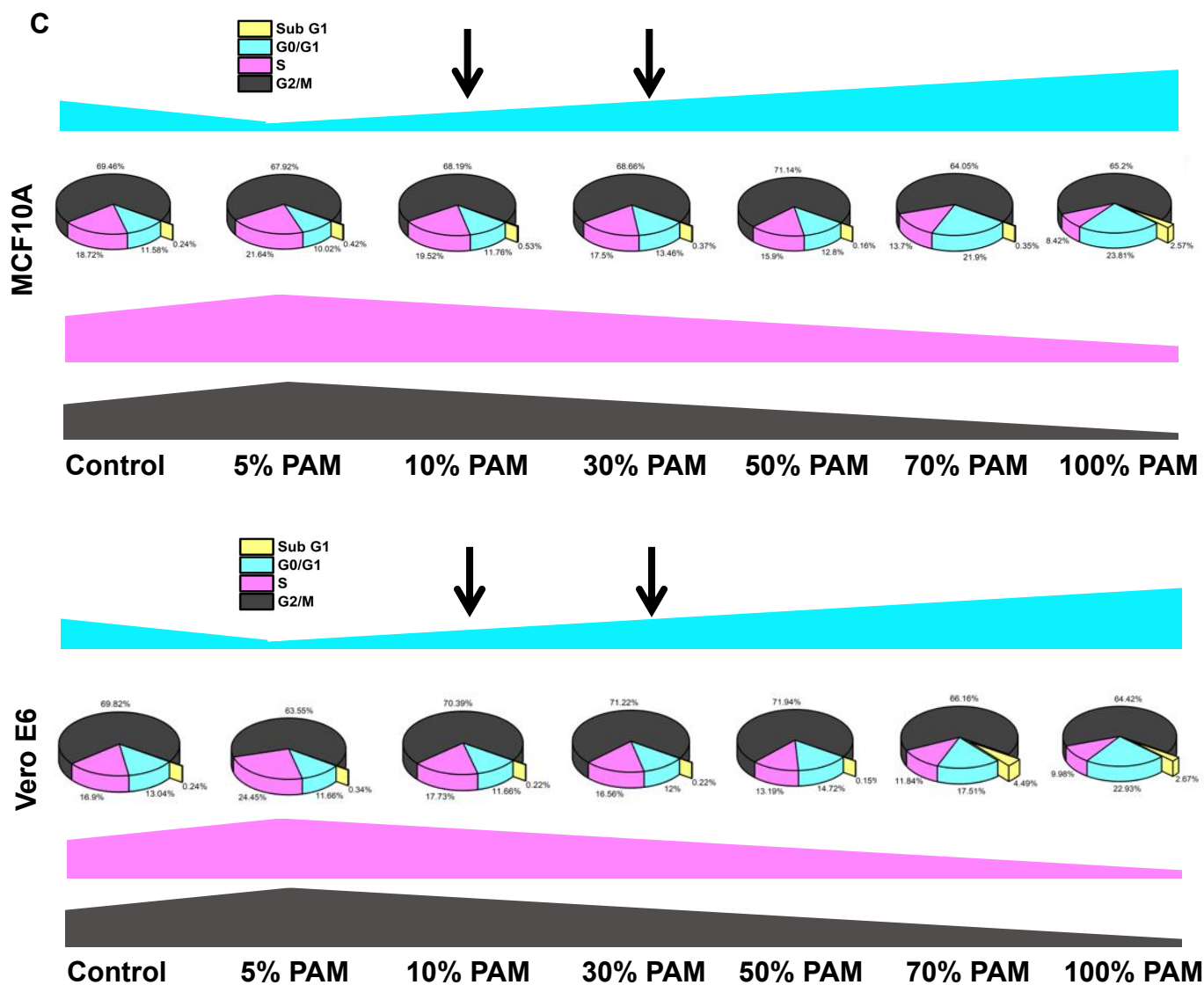
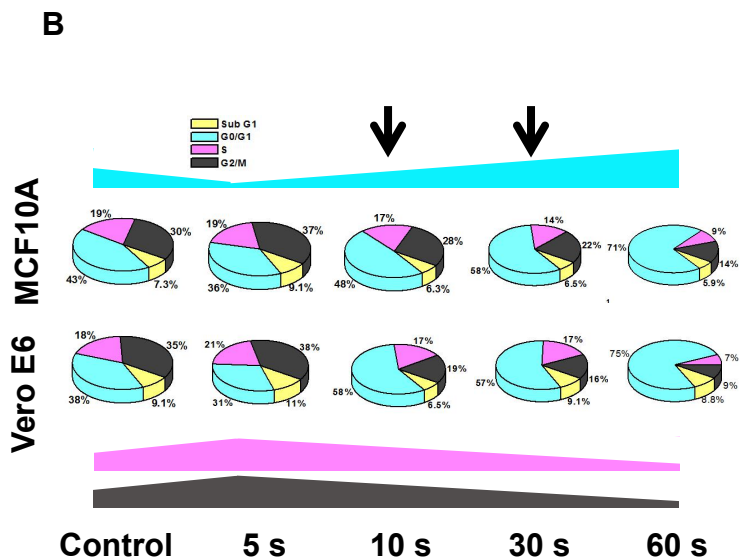
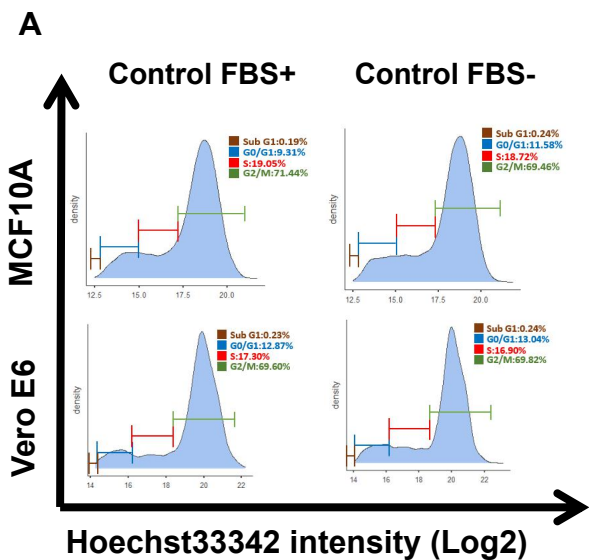


Figure S4. Additional images showing the effects of different CAP and PAM concentrations on cell cycle. (A) Effect of FCS on cell cycle in MCF10A and Vero E6 cells. Cell cycle alteration in response to (B) direct CAP treatment at different treatment durations in MCF10A and Vero E6 cells, and (C) indirect 10-min activated PAM treatment diluted into different concentrations in MCF10A and Vero E6 cells.



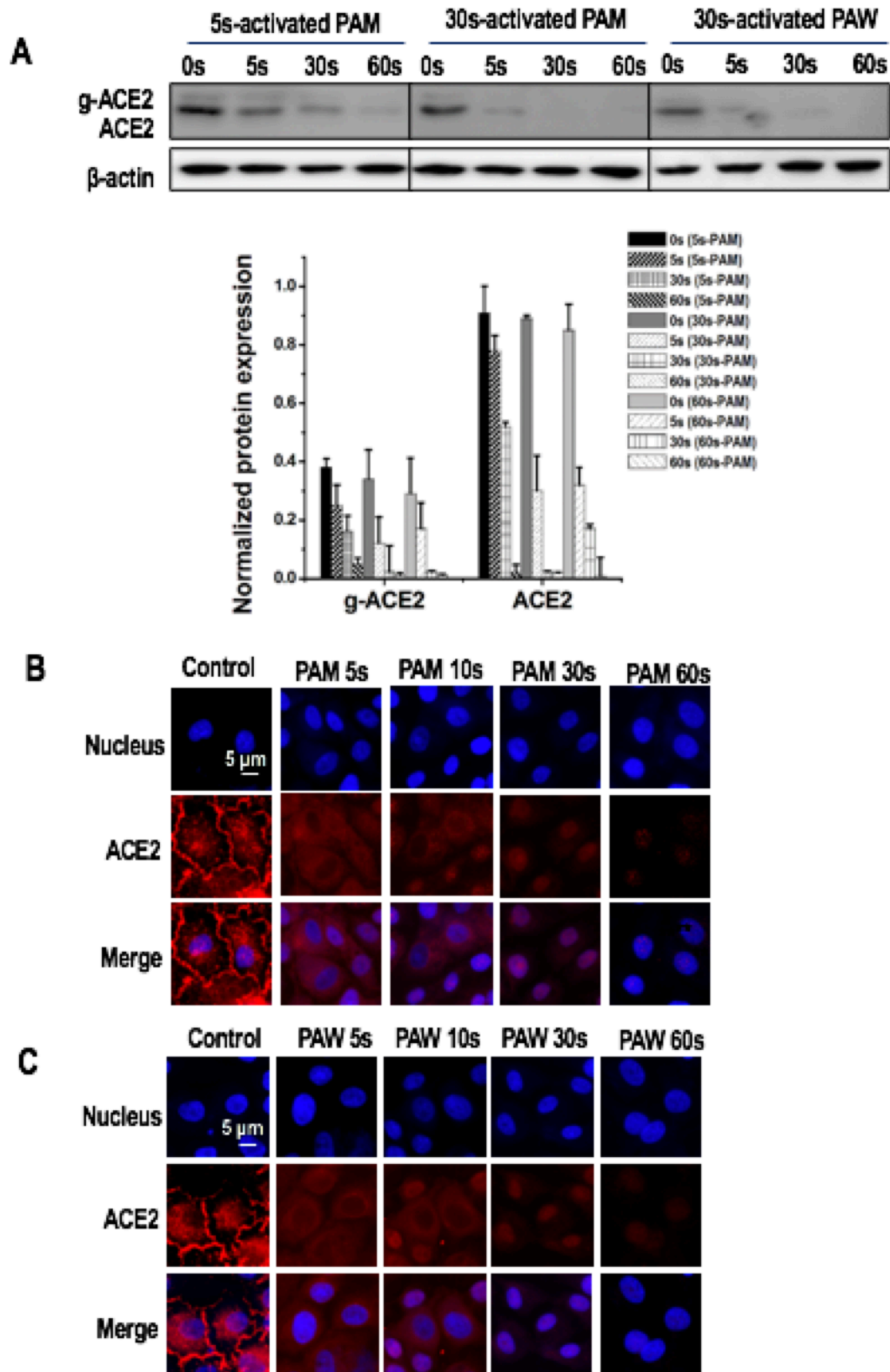


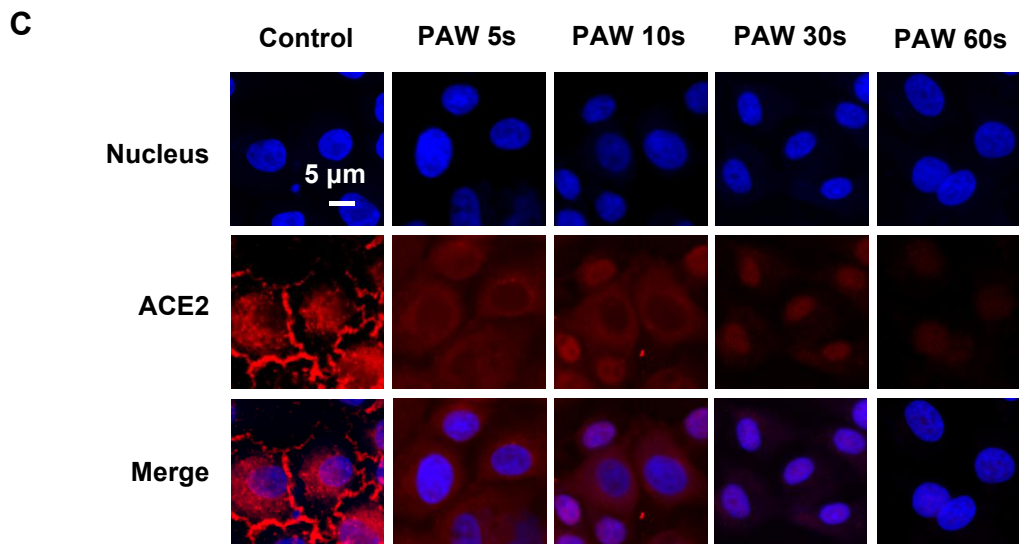
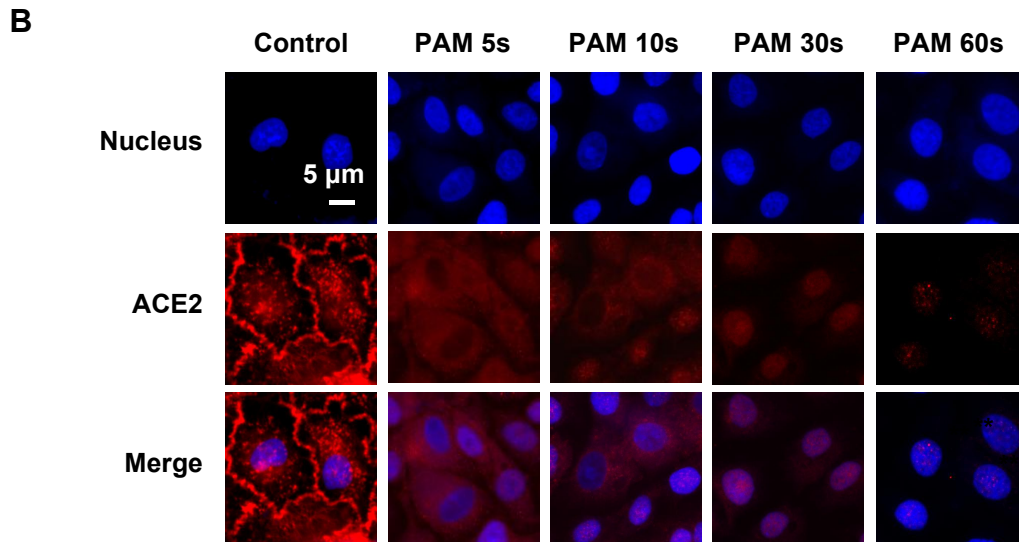
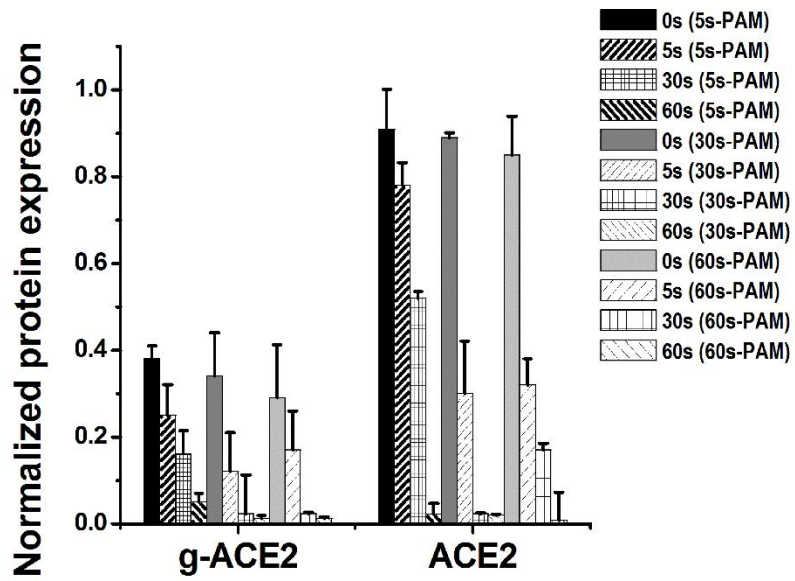
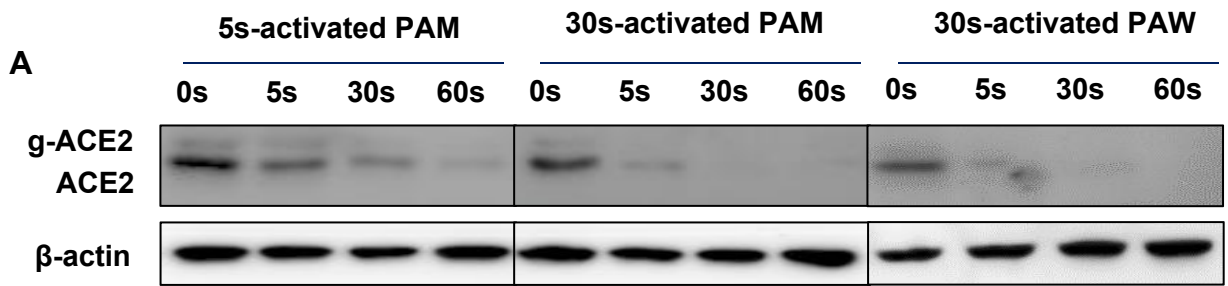
Figure S5. Additional immunofluorescence and Western blots images showing ACE2 expression and cell localization after indirect CAP exposure for different durations.

(A) Western blot of indirect PAM/PAW treatment.

(B) Quantification of ACE2 on indirect PAM/PAW treatment.

(C) Immunofluorescence images of ACE2 on indirect PAM treatment.

(D) Immunofluorescence images of ACE2 on indirect PAW treatment. PAM = plasma activated medium; PAW = plasma activated PBS. MCF10A cells were used. Scale bar=5 μm.



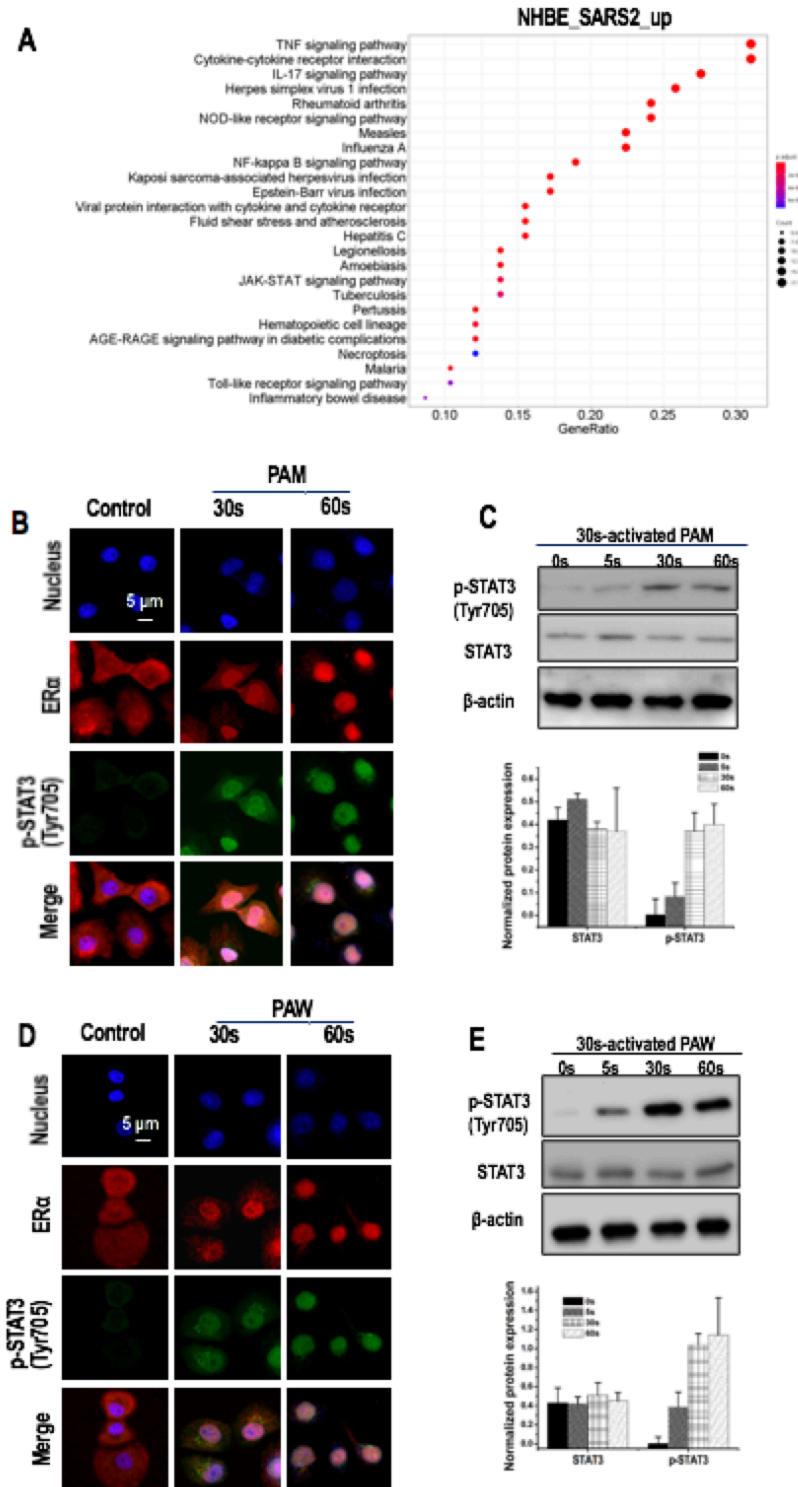


Figure S6. Additional immunofluorescence and western blot images showing ER α and STAT3(Tyr705) expression and cell localization after indirect CAP exposure under different durations.

(A) Up-regulated KEGG pathways enriched by differentially expressed genes in human bronchial epithelial (NHBE) cells on SARS-CoV-2 infection.

(B) Immunofluorescence images showing ER α , phospho-STAT3(Tyr705) location after indirect PAM treatment for different durations.

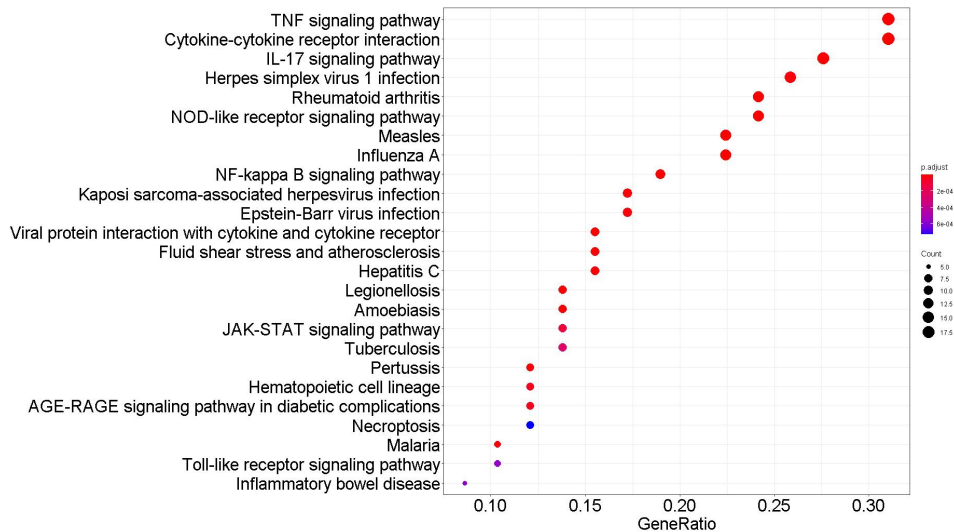
(C) Western blot and quantification showing phospho-STAT3(Tyr705) expression after indirect PAM treatment for different durations.

(D) Immunofluorescence image showing ER α , phospho-STAT3(Tyr705) location after indirect PAW treatment for different durations.

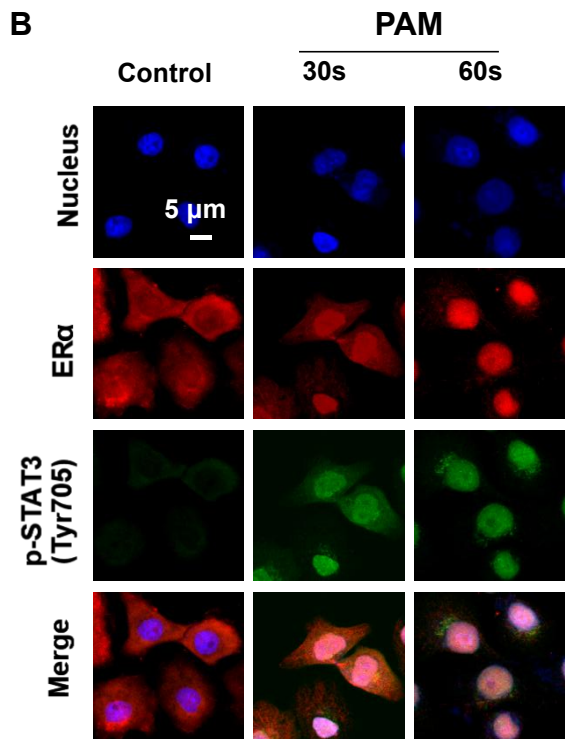
(E) Western blot and quantification showing phospho-STAT3(Tyr705) expression after indirect PAW treatment for different durations. PAM = plasma activated medium; PAW = plasma activated PBS. MCF10A cells were used.

NHBE_SARS2_up

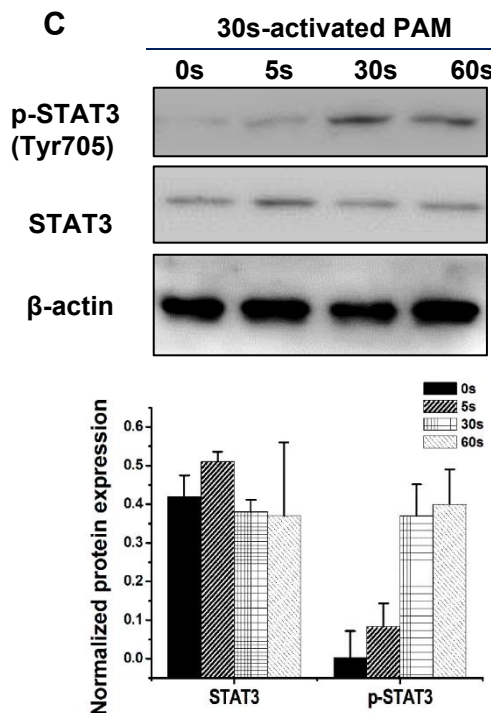
A



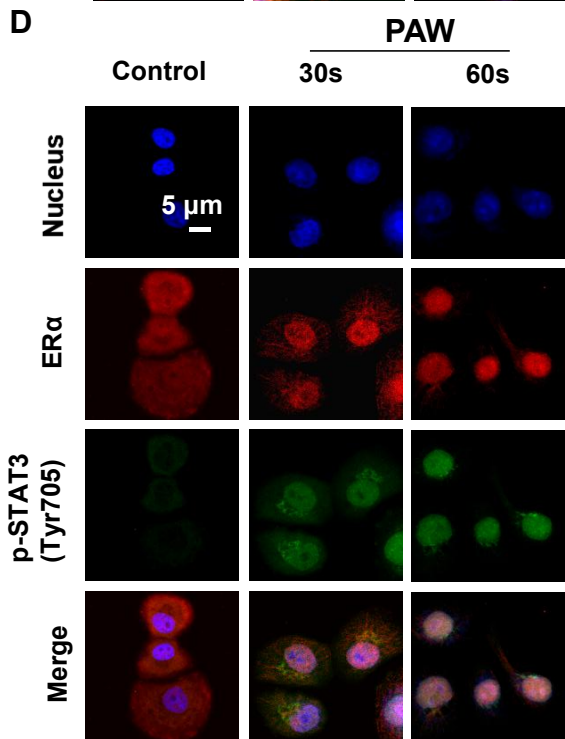
B



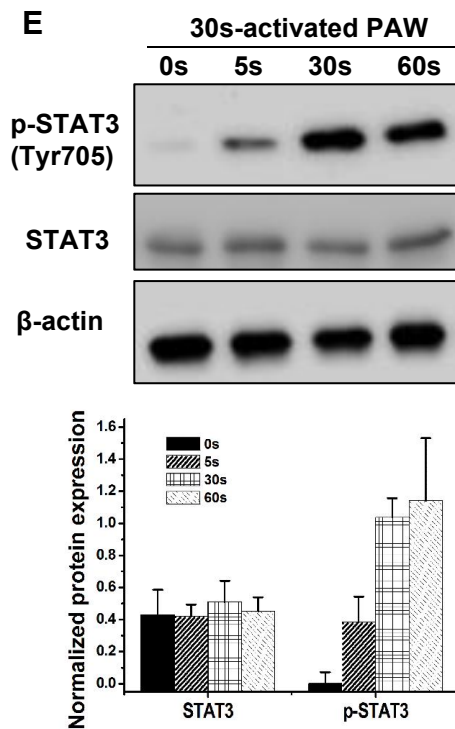
C



D



E



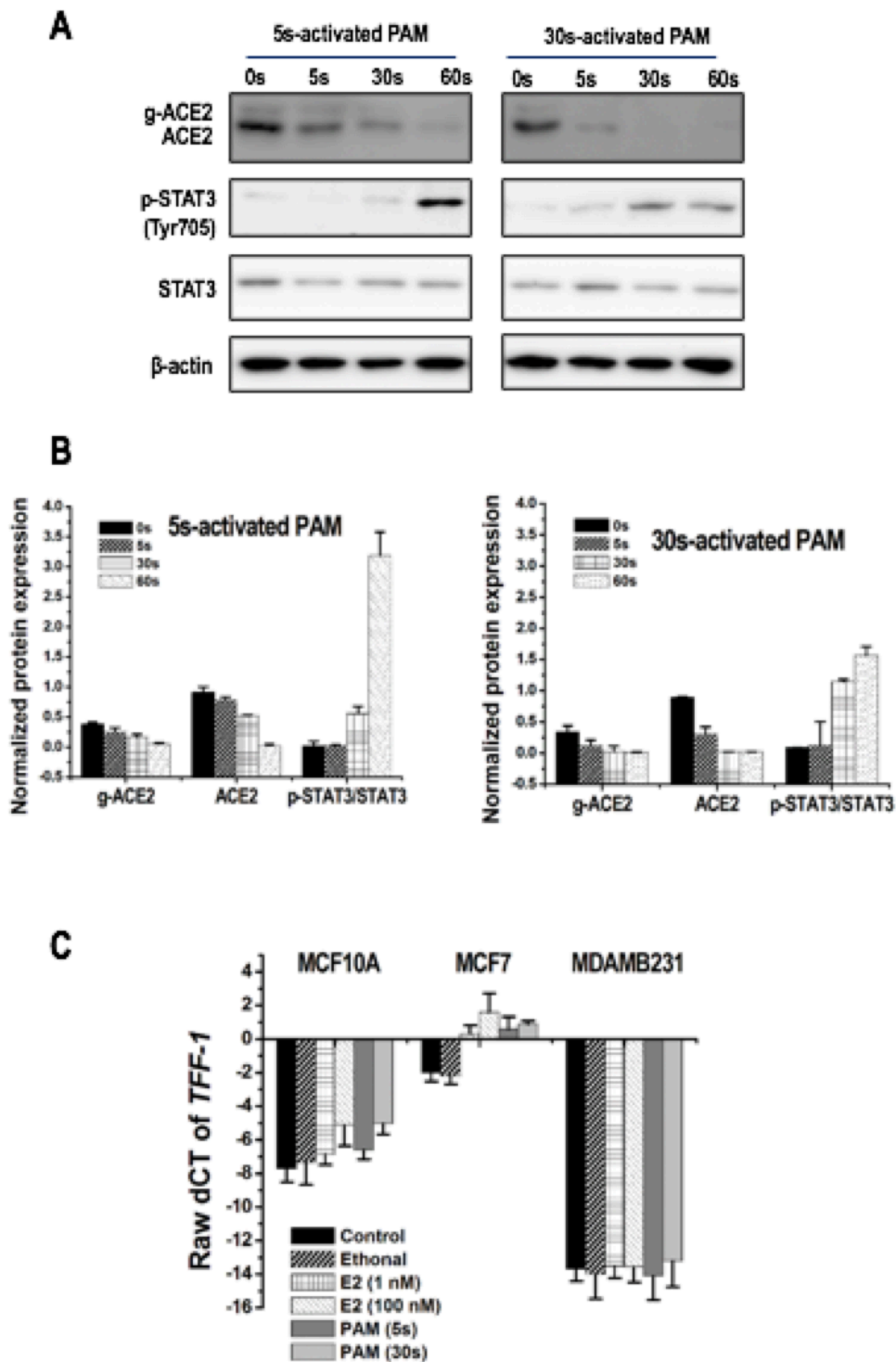
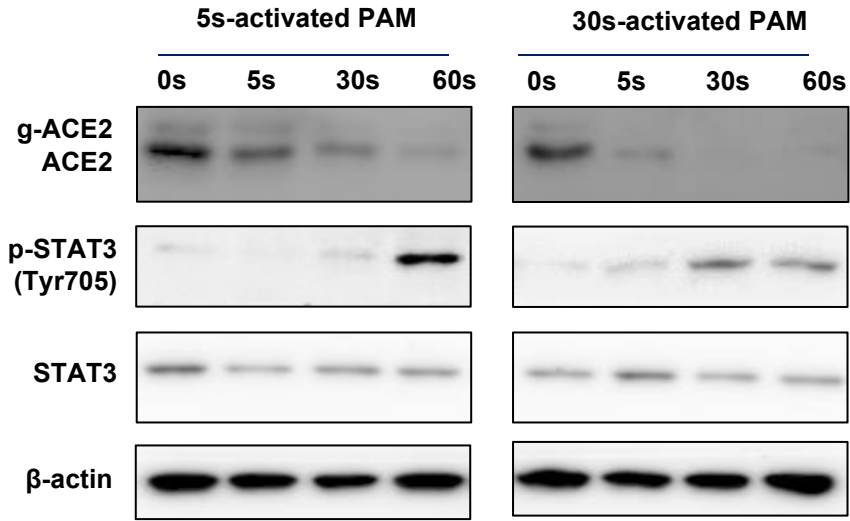
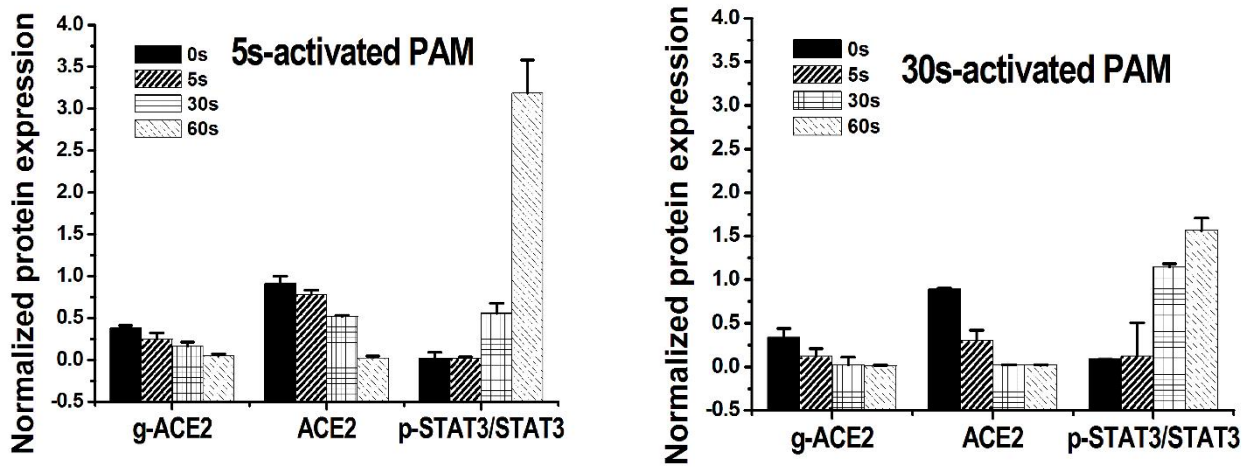
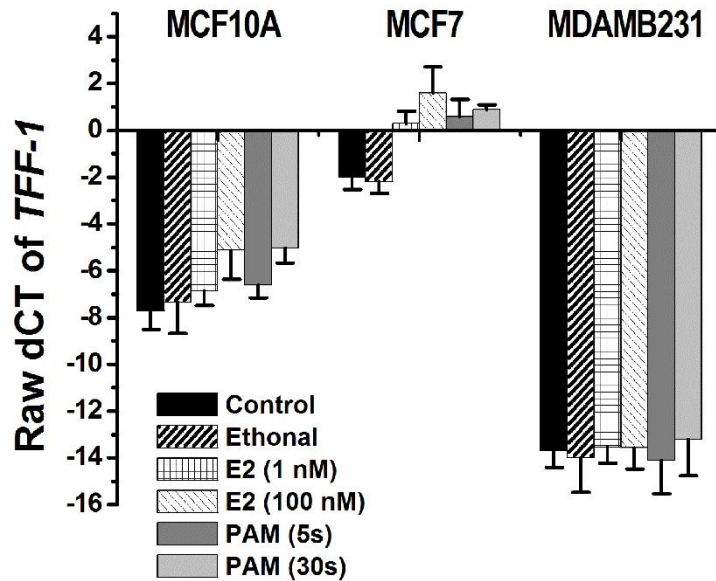


Figure S7. Additional images showing the dosing effect of PAM and estradiol on ACE2 and the ER α /phospho-STAT3(Tyr705) axis. (A) Western blot and (B) quantification of ACE2, STAT3, phospho-STAT3(Tyr705) expression by MCF7 cells incubated with 5 s- and 30 s- activated PAM for different durations. (C) RT-qPCR results showing expression of TFF-1 (a highly sensitive ER-response reporter) after treatment with different doses of PAM and estradiol in MCF10A cells, MDA-MB-231 cells and MCF-7 cells. In (C), TFF-1 raw Ct (cycle threshold) values are defined as the number of cycles required for the fluorescent signal to cross the threshold (*i.e.* exceed background level). Ct levels are inversely proportional to the amount of target nucleic acid in the sample (*i.e.*, the lower the Ct level the greater the amount of target nucleic acid in the sample); a $dCt > 1$ is indicative of abundant target mRNA in the sample; $-10 < dCt < 1$ is indicative of moderate amounts of target mRNA; $dCt < -10$ is indicative of minimal amounts of target mRNA that could be due to environmental contaminations. Ethanol, the solution used for diluting E2, was used as a control in (C). 30 min was used for both E2 and PAM treatment in the RT-PCR testing TFF-1 gene expression.

A**B****C**

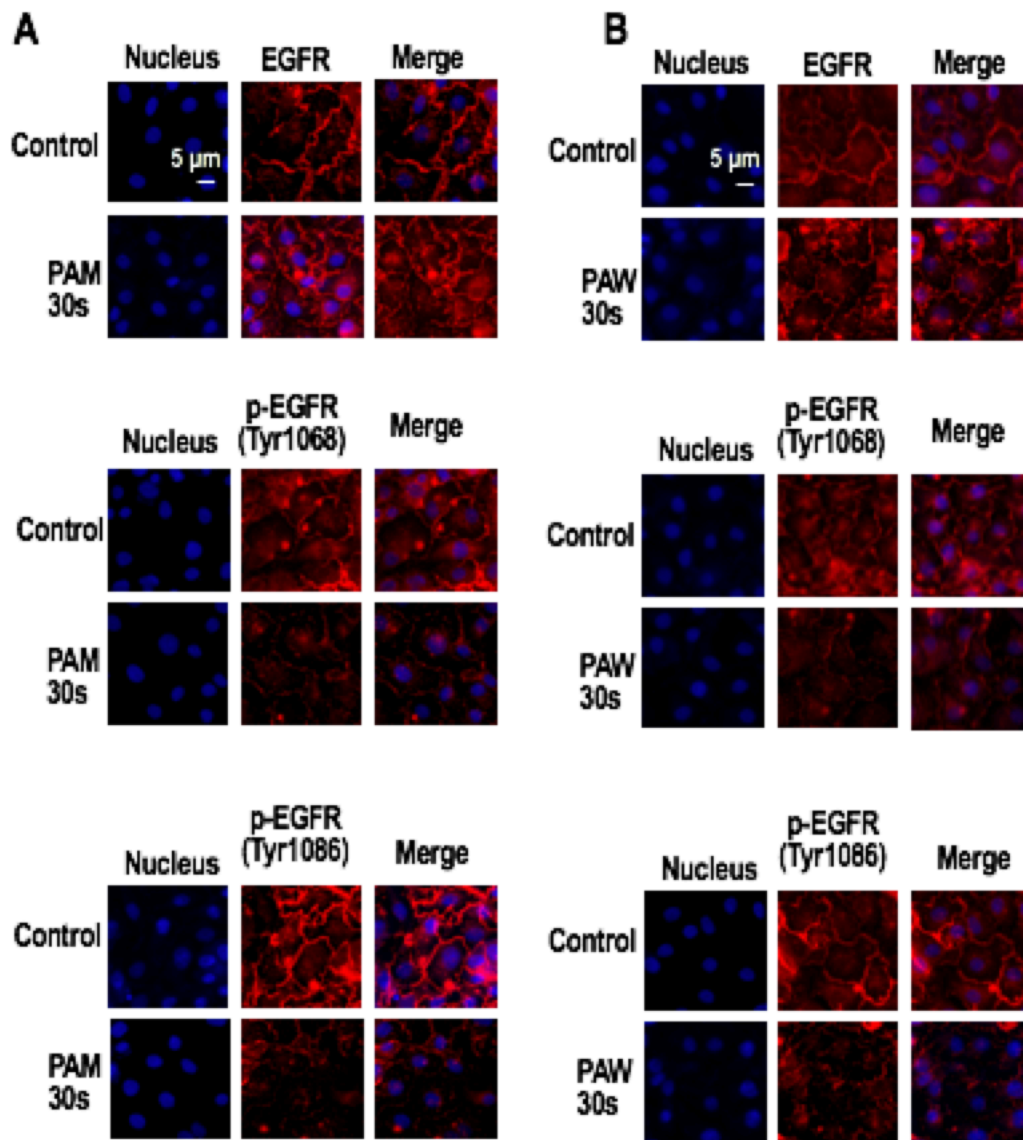


Figure S8. Additional immunofluorescence images showing EGFR(Tyr1068) and EGFR(Tyr1086) expression and cell localization after indirect CAP exposure for 30s. (A) Immunofluorescence image showing EGFR(Tyr1068) and EGFR(Tyr1086) location after indirect (A) PAM and(B), PAW treatment for 30 s. Scale bar=8 μm.

